

Non-equilibrium critical dynamics of the ferromagnetic Ising model with Kawasaki dynamics

Claude Godrèche¹, Florent Krzakala² and Federico Ricci-Tersenghi²

¹ Service de Physique de l'État Condensé, CEA Saclay, 91191 Gif sur Yvette cedex, France

² Dipartimento di Fisica, INFN (UdR Roma I and SMC Centre), Università di Roma 'La Sapienza', P A Moro 2, 00185 Roma, Italy
E-mail: [godreche@spec.saclay.cea.fr](mailto:godreche@spec.saclay cea.fr), Florent.Krzakala@roma1.infn.it and Federico.Ricci@roma1.infn.it

Received 20 January 2004

Accepted 6 April 2004

Published 30 April 2004

Online at stacks.iop.org/JSTAT/2004/P04007

DOI: 10.1088/1742-5468/2004/04/P04007

Abstract. We investigate the temporal evolution of a ferromagnetic system of Ising spins evolving under Kawasaki dynamics from a random initial condition, in spatial dimensions one and two. We examine in detail the asymptotic behaviour of the two-time correlation and response functions. The linear response is measured without applying a field, using a recently proposed algorithm. For the chain at vanishingly small temperature, we introduce an accelerated dynamics which has the virtue of projecting the system into the asymptotic scaling regime. This allows us to revisit critically previous works on the behaviour at large time of the two-time autocorrelation and response functions. We also analyse the case of the two-dimensional system at criticality. A comparison with Glauber dynamics is performed in both dimensionalities, in order to underline the similarities and differences in the phenomenology of the two dynamics.

Keywords: coarsening processes (experiment), coarsening processes (theory), slow dynamics and aging (experiment), slow dynamics and aging (theory)

Contents

1. Introduction	2
2. Measuring the linear response without applying a field in Kawasaki dynamics	3
2.1. Kawasaki dynamics with the heat bath rule	3
2.2. Response function	4
2.3. Computing the linear response in a simulation	5
3. Accelerated dynamics of the Ising–Kawasaki chain in the zero-temperature limit	6
3.1. Rules for the accelerated dynamics	6
3.2. Rules for updating $\Delta\sigma$ during the accelerated dynamics	6
4. Results for the dynamics of the Ising–Kawasaki chain in the zero-temperature limit	7
4.1. Mean domain length	8
4.2. Autocorrelation	9
4.3. Response and fluctuation-dissipation plot	12
5. Results for the critical dynamics of the 2D Ising–Kawasaki model	14
5.1. Mean domain length	14
5.2. Autocorrelation	15
5.3. Response and fluctuation-dissipation plot	17
6. Conclusion	19
Acknowledgments	21
References	21

1. Introduction

The kinetics of ferromagnetic spin systems evolving after an initial quench from a high temperature disordered initial condition to a final temperature, equal to or below the critical temperature, is a well investigated field (see e.g. [1] for a review). However, only recently has the emphasis been put on the dynamics of two-time quantities, such as the correlation and response functions, or the fluctuation-dissipation violation ratio, with the aim of quantifying the distance of the system from equilibrium during its temporal evolution [2]–[18] (see e.g. [19] for a brief review). Most of these studies focus on the non-conserved order parameter case, where at each time step a single spin is updated according to the rules of Glauber dynamics. An overall coherent picture of this field has now emerged, though some controversies remain [20]–[23].

Far fewer studies have been devoted so far to the same questions, namely the temporal evolution of two-time quantities, for the case of conserved order parameter dynamics. Restricting to a system of discrete spins, the rules of Kawasaki dynamics [24] now consist in choosing two adjacent opposite spins, and exchanging them with a rate depending on the energy difference between the initial and final configurations. In the recent past the question of the long time behaviour of the autocorrelation function for conserved

dynamics has already been addressed [25, 26, 28]. In particular predictions have been given for the values of the autocorrelation exponents λ and λ_c governing the decay of the autocorrelation function at large temporal separations, respectively in the low temperature phase and at criticality. Finally, a very recent work addresses the question of the response for the Ising–Kawasaki chain in the low temperature scaling regime [29]. The prediction made in this reference states that the fluctuation-dissipation plot (that is the relationship between integrated response and correlation) of this case is identical to that of the Glauber non-conserved case, which is itself known analytically [8, 9]. This result is rather surprising because it would imply some kind of ‘super-universal’ behaviour in the relationship between correlation and response in the asymptotic regime.

The aim of the present work is to revisit and extend these former studies. We investigate the behaviour of the two-time correlation and response functions for an Ising spin system, both in one and two dimensions, with Hamiltonian

$$\mathcal{H} = - \sum_{\langle i,j \rangle} \sigma_i \sigma_j, \quad (1)$$

where $\langle i, j \rangle$ are nearest neighbours, evolving under Kawasaki dynamics after a quench of the system from a disordered high temperature initial condition to the critical temperature.

We first give the method used in this paper in order to compute the linear response. This method, due to Chatelain [30], and later on clarified in [31], will be used both for the one-dimensional and two-dimensional cases. We then describe the rules of an accelerated dynamics for the Ising–Kawasaki chain corresponding to the formal limit $T \rightarrow 0$, which is nevertheless faithful, i.e. reproduces exactly the results that would be obtained with the usual rules of Kawasaki dynamics for vanishingly small temperatures. We finally present the results of extensive numerical computations of the autocorrelation and response functions, first for the case of a chain, then for the two-dimensional system at criticality.

2. Measuring the linear response without applying a field in Kawasaki dynamics

In this section we give an analytical expression for the response function to an infinitesimal field, for a ferromagnetic system evolving under Kawasaki dynamics, and show how this quantity can be measured. We follow the lines of reasoning of [30, 31], which are devoted to the same question for single-spin-flip dynamics.

2.1. Kawasaki dynamics with the heat bath rule

Hereafter, time t is discrete and counts the number of spin exchange attempts, and not the number of Monte Carlo sweeps. In order to define a response function, an external perturbing field h_i is applied on any site i , and, in the presence of the field, the Hamiltonian is changed to $\mathcal{H} - \sum h_i \sigma_i$.

Kawasaki rules consist in updating a pair of two opposite adjacent spins $\sigma_i = -\sigma_j$ (we will always omit the $\delta_{\sigma_i, -\sigma_j}$ factor in the following), with heat bath probabilities

$$\mathcal{P}(\sigma_i = \sigma, \sigma_j = -\sigma) = \frac{\exp[\beta\sigma(h_{ij}^W + h_i - h_j)]}{2 \cosh[\beta(h_{ij}^W + h_i - h_j)]}, \quad (2)$$

where β is the inverse temperature, and the Weiss field h_{ij}^W takes into account the effect of neighbours on the couple of spins which are updated. For a generic two-spin interaction Hamiltonian we have

$$h_{ij}^W = \sum_{k \in \partial i \setminus j} J_{ik} \sigma_k - \sum_{l \in \partial j \setminus i} J_{jl} \sigma_l, \quad (3)$$

where $\partial i \setminus j$ represents the set of neighbours of i , with j excluded. For example, in one dimension, with Hamiltonian (1), we have $h_{i,i+1}^W = \sigma_{i-1} - \sigma_{i+2}$.

2.2. Response function

Following strictly the notation of [31], we consider systems made of N Ising spins, where the autocorrelation and the response functions are defined as

$$C(t, s) = \frac{1}{N} \sum_{i=1}^N \langle \sigma_i(t) \sigma_i(s) \rangle, \quad R(t, s) = \frac{1}{N} \sum_{i=1}^N \frac{\partial \langle \sigma_i(t) \rangle}{\partial h_i(s)}, \quad (4)$$

with $\langle \cdot \rangle$ representing the average over thermal histories.

We concentrate on the integrated response function, or susceptibility

$$\chi(t, s) = T \int_s^t du R(t, u), \quad (5)$$

where the temperature T has been added in the usual definition in order to simplify the notation and to have a well defined expression in the $T \rightarrow 0$ limit.

Denoting by $I(t)$ and $J(t)$ the indices of the two spins to be updated at time t , the expectation value of the k th spin at time t is given by

$$\langle \sigma_k(t) \rangle = \text{Tr}_{\vec{\sigma}(t')} \left[\sigma_k(t) \prod_{t'=1}^t W_{I(t')J(t')}(\vec{\sigma}(t') | \vec{\sigma}(t' - 1)) \right], \quad (6)$$

where $\vec{\sigma}$ is the vector of the N -spin configuration, the trace is over all the histories $\vec{\sigma}(t')$, with $1 \leq t' \leq t$, and the transition probabilities are given by

$$W_{ij}(\vec{\sigma} | \vec{\tau}) = \frac{\exp[\beta \sigma_i (h_{ij}^W + h_i - h_j)]}{2 \cosh[\beta (h_{ij}^W + h_i - h_j)]} \prod_{k \neq i, j} \delta_{\sigma_k, \tau_k}. \quad (7)$$

Note that $h_{ij}^W(\vec{\sigma}) = h_{ij}^W(\vec{\tau})$, because the Weiss field does not depend on the value of the spins at sites i and j . Since the transition probability W_{ij} only depends on the perturbing fields on sites i and j , one has

$$\left. \frac{\partial W_{ij}(\vec{\sigma} | \vec{\tau})}{\partial h_k} \right|_{h=0} = \beta W_{ij}(\vec{\sigma} | \vec{\tau}) [\delta_{i,k} (\sigma_i - \sigma_{ij}^W) + \delta_{j,k} (\sigma_j + \sigma_{ij}^W)], \quad (8)$$

where we have defined $\sigma_{ij}^W \equiv \tanh(\beta h_{ij}^W)$.

Now, if on site k an infinitesimal probing field h_k is switched on at time s (i.e. $h_k(t) = h\theta(t - s)$), all transition probabilities with index k (and only these ones) will depend on

the perturbing field for times larger than s . Then differentiation of equation (6) with respect to this field yields the integrated response

$$\chi_{lk}(t, s) = T \left. \frac{\partial \langle \sigma_l(t) \rangle}{\partial h_k} \right|_{h=0} = \text{Tr}_{\vec{\sigma}(t')} \left[\sigma_l(t) \prod_{t'=1}^t W_{I(t'), J(t')}(\vec{\sigma}(t') | \vec{\sigma}(t' - 1)) \right. \\ \left. \times \sum_{u=s+1}^t [\delta_{I(u), k}(\sigma_k(u) - \sigma_{I(u)J(u)}^W(u)) + \delta_{J(u), k}(\sigma_k(u) + \sigma_{I(u)J(u)}^W(u))] \right] \quad (9)$$

which can be simply written as a correlation function

$$\chi_{lk}(t, s) = \langle \sigma_l(t) \Delta \sigma_k(t, s) \rangle, \quad (10)$$

where

$$\Delta \sigma_k(t, s) = \sum_{u=s+1}^t \delta_{I(u), k}[\sigma_k(u) - \sigma_{I(u)J(u)}^W(u)] + \delta_{J(u), k}[\sigma_k(u) + \sigma_{I(u)J(u)}^W(u)]. \quad (11)$$

2.3. Computing the linear response in a simulation

Let us note that calculating the linear response in a numerical simulation with no perturbing field using equation (10) is as easy as measuring a correlation function. One has to keep track of the vector $\Delta \sigma_k(t, s)$ that should be updated for all times between s and t (i.e. when the ‘ghost’ field is switched on). At each of these times, one has to:

- compute h_{ij}^W and $\sigma_{ij}^W \equiv \tanh(\beta h_{ij}^W)$;
- update spins σ_i and σ_j according to the heat bath probability (with no external field)

$$\mathcal{P}(\sigma_i = \sigma, \sigma_j = -\sigma) = \frac{\exp(\beta \sigma h_{ij}^W)}{2 \cosh(\beta \sigma h_{ij}^W)};$$

- increment $\Delta \sigma_i, \Delta \sigma_j$ as

$$\Delta \sigma_i \rightarrow \Delta \sigma_i + \sigma_i - \sigma_{ij}^W, \quad (12)$$

$$\Delta \sigma_j \rightarrow \Delta \sigma_j + \sigma_j + \sigma_{ij}^W. \quad (13)$$

It is important to note at this point that contributions to the increment $\Delta \sigma_i$ come either when the updated spin flips or *when it does not*, keeping its previous value. This is why one can speak of a ‘ghost’ field in this method (see above). An illustration of this is encountered in section 3.2 below.

The use of equation (10) allows one to compute, in a single run, the integrated response (5) (zero-field cooled magnetization), as well as the thermoremanent magnetization,

$$\rho(t, s) = T \int_0^s du R(t, u), \quad (14)$$

both for many different values of s .

3. Accelerated dynamics of the Ising–Kawasaki chain in the zero-temperature limit

It is well known that the Kawasaki dynamics at zero temperature rapidly brings the one-dimensional system to a blocked state, where the distance between any couple of domain walls is at least 2 [32, 33]. In such a situation any spin exchange move would cost an energy $\Delta E = 4$, and is therefore forbidden. For example $\uparrow\uparrow\uparrow\uparrow\downarrow\downarrow\downarrow\downarrow \rightarrow \uparrow\uparrow\uparrow\downarrow\uparrow\downarrow\downarrow\downarrow$ would create two domain walls. Such a process is called an *evaporation* [32].

However, at an infinitesimal temperature $T = \varepsilon$, the evolution may eventually undergo such an evaporation with probability $1/(1 + e^{4/\varepsilon})$, hence on a timescale $O(e^{4/\varepsilon})$, which diverges for $\varepsilon \rightarrow 0$. After each evaporation process the dynamics proceeds by *diffusion*, that is by moves with energy cost $\Delta E = 0$ (e.g. $\downarrow\downarrow\downarrow\uparrow\downarrow\downarrow\downarrow \rightarrow \downarrow\downarrow\downarrow\uparrow\downarrow\downarrow\downarrow$), until a *condensation* process occurs, corresponding to a move with energy cost $\Delta E = -4$, which brings the system back to a new blocked state (e.g. $\downarrow\downarrow\downarrow\uparrow\downarrow\uparrow\uparrow \rightarrow \downarrow\downarrow\downarrow\uparrow\uparrow\uparrow$). The diffusion and condensation processes take place on scales of time $O(1)$, i.e. much smaller than the typical time between two consecutive evaporations, and therefore can be considered as instantaneous if time is counted in units of $\tau = e^{4/\varepsilon}$, when $\varepsilon \rightarrow 0$.

We exploit the strong separation of timescales between evaporation and diffusion/condensation processes, and we simulate the dynamics of the Ising–Kawasaki chain in the limit $T = \varepsilon \rightarrow 0$ with the following accelerated dynamics. Time in this accelerated dynamics is counted in units of $\tau = e^{4/\varepsilon}$.

3.1. Rules for the accelerated dynamics

As long as the system is not in a blocked state, we use the usual $T = 0$ Kawasaki dynamics where only spin exchanges with $\Delta E \leq 0$ are accepted. During these lengths of time, since the only processes occurring, diffusion and condensation, are actually instantaneous on the scale $\tau = e^{4/\varepsilon}$, time is not increased at all.

When the system is in a blocked state (with a number n of domain walls), we choose randomly a domain wall, we exchange the two spins on the sides of the domain wall (evaporation), and we increase the time by $\Delta t = 1/n$.

The choice for Δt can be understood as follows. In a Monte Carlo simulation at $T = \varepsilon$, the probability of accepting an evaporation process being approximately equal to $e^{-4/\varepsilon}$, on average, a number $O(e^{4/\varepsilon})$ of tries will be necessary before a success. In each Monte Carlo sweep (MCS) n tries are made, since the only couples of spins which satisfy the requirement $\sigma_i = -\sigma_j$ are those around a domain wall. Thus the typical number of MCS done before an evaporation process takes place is τ/n , i.e. $\Delta t = 1/n$ in units of τ .

3.2. Rules for updating $\Delta\sigma$ during the accelerated dynamics

Being a quantity integrated over time, $\Delta\sigma_k(t, s)$ has contributions from both fast and slow processes.

Moreover, for $T \rightarrow 0$, equations (12) and (13) can be simplified to $\Delta\sigma_i \rightarrow \Delta\sigma_i + \{2\sigma_i, \sigma_i, 0\}$ and $\Delta\sigma_j \rightarrow \Delta\sigma_j + \{2\sigma_j, \sigma_j, 0\}$, respectively, for evaporation, diffusion, and condensation processes.

Between two evaporation processes, there is however an additional contribution to take into account (see equation (17) below), which is not apparent in equations (12) and (13). This is a direct consequence of the fact, mentioned above, that $\Delta\sigma_k(t, s)$

has contributions from updated spins, even when they do not flip. Consider a blocked configuration, where all the spins are aligned with their local fields, $\sigma_i = \text{sgn}(h_{ij}^W)$ and $\sigma_j = -\text{sgn}(h_{ij}^W)$. Since the time spent in each blocked state becomes infinite for $\varepsilon \rightarrow 0$, a non-trivial limit for the integrated quantity $\Delta\sigma$ is generated. Indeed, working at temperature $T = \varepsilon$ and noting that in a blocked state $h_{ij}^W = 2\sigma_i$, we have

$$\sigma_{ij}^W = \tanh(h_{ij}^W/\varepsilon) \approx \text{sgn}(h_{ij}^W)[1 - 2e^{-2|h_{ij}^W|/\varepsilon}] = \sigma_i \left(1 - \frac{2}{\tau}\right); \quad (15)$$

hence,

$$\sigma_i - \sigma_{ij}^W \approx \frac{2\sigma_i}{\tau}. \quad (16)$$

Then the summation over τ/n MCS of the last quantity gives a finite limit when $\varepsilon \rightarrow 0$ and $\tau \rightarrow \infty$. In practice this means that, just before leaving a blocked state by an evaporation process, all the $\Delta\sigma_i$ for spins close to a domain wall must be updated with the following rule:

$$\Delta\sigma_i \rightarrow \Delta\sigma_i + \frac{2\sigma_i}{n}. \quad (17)$$

Some final comments on the accelerated dynamics described in this section are in order.

- This dynamics is faithful, i.e. it reproduces *exactly* the results that would be obtained by a standard Monte Carlo simulation at finite temperature $T = \varepsilon$, in the limit $\varepsilon \rightarrow 0$. This equivalence will be illustrated below on the example of the mean length of domains. It is also very efficient, since it requires much less computational effort than the standard Monte Carlo dynamics.
- Its definition can be extended to any spatial dimension.
- Finally, one may wonder how this dynamics compares to the effective dynamics of [32, 34], which is only defined in one dimension. The spirit of the latter is to trace over all events occurring between the instant of time when a spin detaches from a domain and that when it reaches the neighbouring domain. The accelerated dynamics introduced in this section does not trace over these events. However, doing so—in one dimension only—would lead to the dynamics of [32, 34], and allow a faster computation of the average domain length $L(t)$, and with little more work, of the autocorrelation. In contrast, tracing over these events is much more subtle for the computation of the response, and would deserve further study. Otherwise stated, it is not clear to us for the time being whether the method of [32, 34] can be used for the computation of the response. The difficulty comes from the fact that $\Delta\sigma$ has contributions even when spins are updated without changing their value.

4. Results for the dynamics of the Ising–Kawasaki chain in the zero-temperature limit

In this section we report the results of extensive numerical simulations, using the methods described in the previous sections. We are interested in the behaviour of observables in the

Non-equilibrium critical dynamics of the ferromagnetic Ising model with Kawasaki dynamics

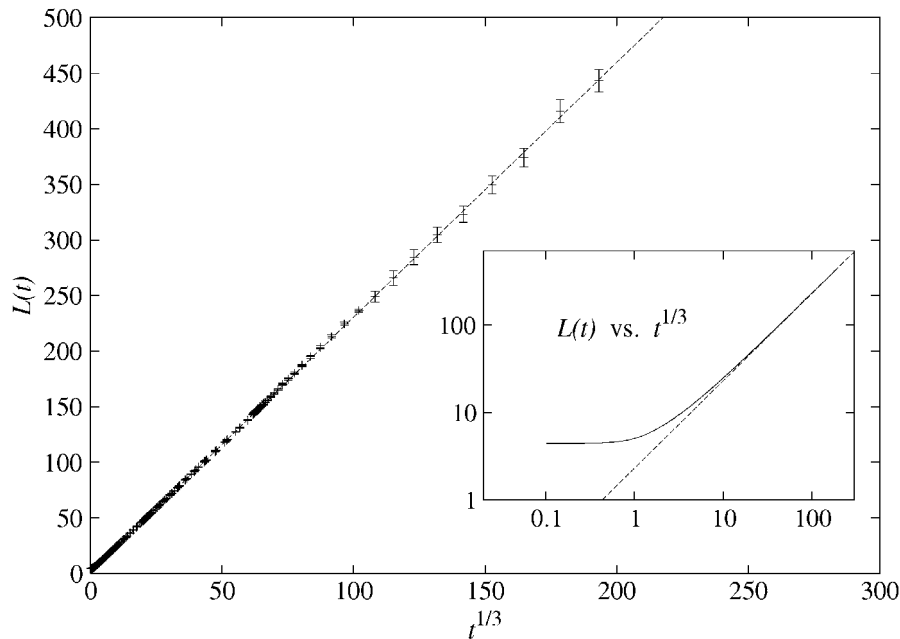


Figure 1. Mean domain length $L(t)$ against $t^{1/3}$ for the Ising–Kawasaki chain obtained with the accelerated dynamics for vanishingly small temperature. Inset: the same data on a log–log scale.

low temperature scaling regime defined by $1 \ll t \ll t_{\text{eq}}$, where the equilibration time t_{eq} is related, at inverse temperature $\beta = 1/\varepsilon$, to the equilibrium correlation length $\xi \approx e^{2\beta}/2$ by $t_{\text{eq}} \sim \xi^5$ [35]. This regime is naturally attained by the accelerated dynamics.

4.1. Mean domain length

The mean domain length is related to the energy $E(t)$ of the chain at time t by

$$L(t) = \frac{2}{1 + E(t)}. \quad (18)$$

It is well known that, in the low temperature scaling regime, $L(t)$ scales as

$$L(t) \sim \left(\frac{t}{\tau}\right)^{1/3}, \quad (19)$$

where $\tau = e^{4\beta} \sim \xi^2$. This scaling is illustrated in [35], where for increasing values of τ (i.e. decreasing temperatures) a linear master curve is found when $L(t)$ is plotted against $(t/\tau)^{1/3}$.

We measured $L(t)$ using the accelerated dynamics of section 3. Since time is measured in units of τ in such a scheme, the curve thus found is the limiting master curve that would have been found by the conventional means of [35] in the limit $T \rightarrow 0$. We did indeed check that the amplitude of the law (19), $L(t) = A (t/\tau)^{1/3}$, found in [35] was in agreement with, though less precise than, that found in the present work, $A \simeq 2.29$. Figure 1 depicts the master curve thus obtained in the $T \rightarrow 0$ limit. The system size is $N = 2^{12} = 4096$,

Table 1. For each choice of the number of evaporation processes before the measurement of the autocorrelation and response, the corresponding value of the waiting time s and the number of different thermal histories are reported.

No of evap.	0	10^3	10^4	10^5	10^6	10^7
s value	0^+	1.1710(5)	15.998(12)	312.43(23)	8000(9)	235 580(740)
No of samp.	895	1189	717	1146	1179	51

and the numbers of samples are reported in table 1. (We also checked for the absence of any finite-size effects by simulating a few $N = 2^{16}$ samples.)

The inset of figure 1 shows the growth of $L(t)$ in a log–log scale. The convergence to the slope $1/3$ is slow, mainly because of the presence of an offset at initial times. This offset corresponds to the first blocked state reached by the system. Recall that the system is prepared at time $t = 0$ in a random configuration. It then evolves under $T = 0$ Kawasaki dynamics, until it reaches the first blocked state at time $t = 0^+$ in units of τ . This first blocked state has a mean domain length $L(0^+) = 4.158\,86(15)$.

4.2. Autocorrelation

A well known fact of the kinetics of coarsening with non-conserved dynamics is that, in the low temperature scaling regime, and for large temporal separations ($1 \ll s \ll t \ll t_{\text{eq}}$), the two-time autocorrelation $C(t, s)$ decays as [1]

$$C(t, s) \sim \left(\frac{L(t)}{L(s)} \right)^{-\lambda}, \quad (20)$$

and, for the particular case where $s = 0$, as

$$C(t, 0) \sim L(t)^{-\lambda}, \quad (21)$$

defining the autocorrelation exponent λ [36].

The case of conserved dynamics is more complex. For quenches to temperatures below T_c , Yeung *et al* [28] find bounds on the autocorrelation exponent which depend on the value of the smallest time s . For $s = 0$, $\lambda \geq d/2$, where d is the dimensionality of space, while for values of s in the scaling regime, $\lambda \geq d/2 + 2$ for $d \geq 2$ and $\lambda \geq 3/2$ for $d = 1$.

Given the prediction of [25] that, in the low temperature phase, $C(t, 0) \sim L(t)^{-\lambda}$, with $\lambda = d$, Yeung *et al* conclude that, for $d = 1$ (and more generally for low dimensions), the behaviour (21) holds for s small, while for s in the scaling regime the behaviour (20) should be replaced by

$$C(t, s) \sim \left(\frac{L(t)}{L(s)} \right)^{-\lambda'} \quad (22)$$

with a different exponent $\lambda' > \lambda$.

The prediction above therefore implies that for the Ising–Kawasaki chain at vanishingly small temperature the curves of the autocorrelation for two values of s , one being taken in the short time regime, the other one in the scaling regime, should cross at some later time t^* . This simple observation was not noticed by the authors of [28]. The

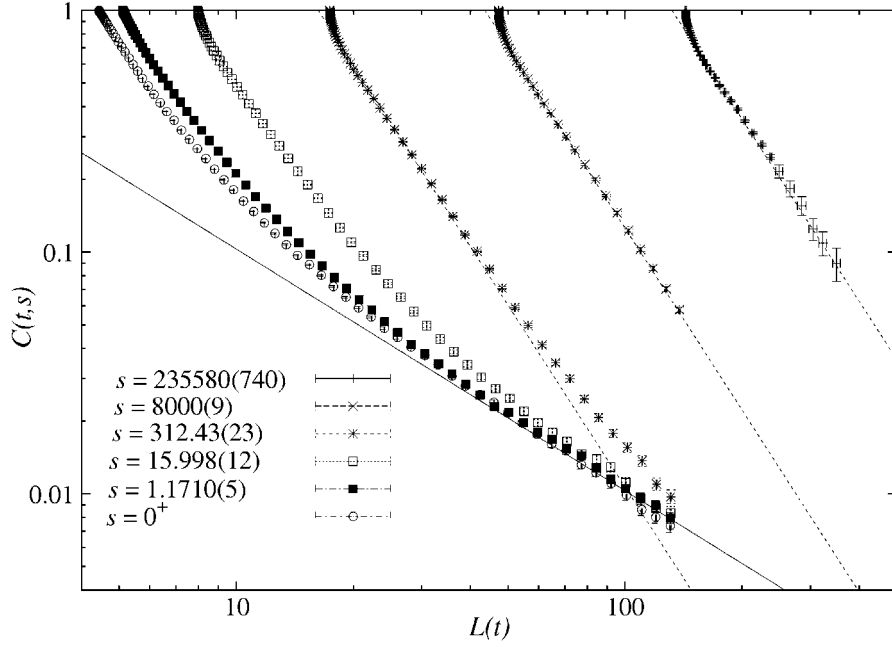


Figure 2. The two-time autocorrelation function of the Ising–Kawasaki chain at vanishingly small temperature. The full line has slope $-\lambda = -1$, while the dotted ones have slope $-\lambda' = -2.5$.

question therefore arises of what is the behaviour of the autocorrelation $C(t, s)$ for later times $t \gg t^*$.

Hereafter we suggest the following scenario, based on the reasonable hypothesis that the two curves mentioned above do not cross. Define more precisely $t^*(s)$ by

$$L(t^*)^{-\lambda} \sim \left(\frac{L(t^*)}{L(s)} \right)^{-\lambda'}, \quad (23)$$

i.e. $t^*(s) \sim s^{\lambda'/(\lambda'-\lambda)}$. Then, there are two scaling regimes:

- the intermediate scaling regime of Yeung *et al*, for $t \ll t^*$, where (22) holds;
- the ultimate scaling regime, for $t \gg t^*$, where

$$C(t, s) \sim L(t)^{-\lambda}. \quad (24)$$

Therefore the following scaling law should hold:

$$C(t, s) = L(t)^{-\lambda} g \left(\frac{L(t)^{\lambda'-\lambda}}{L(s)^{\lambda'}} \right), \quad (25)$$

with $g(x \rightarrow 0) \sim x^{-1}$ in the intermediate regime, while in the ultimate regime $g(x \rightarrow \infty)$ should converge to a constant.

Outcomes from our simulations are compatible with these predictions. Figure 2 shows the autocorrelation function as a function of $L(t)$, for the values of s given in table 1. The presence of two different scaling regimes is evident, although the intermediate regime is

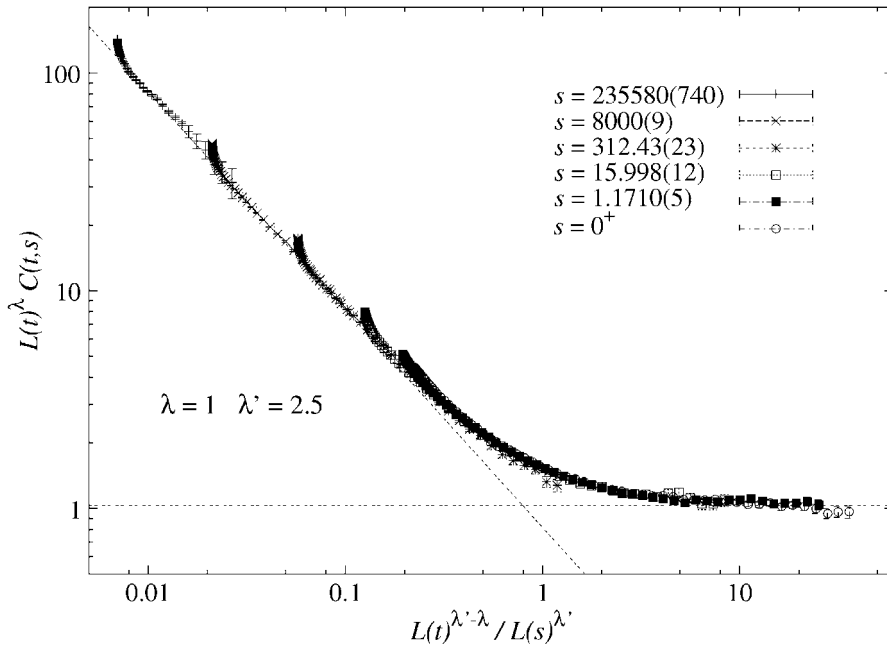


Figure 3. The scaling function for the two-time autocorrelation of the Ising–Kawasaki chain at vanishingly small temperature (see the text).

not very clean for small s data, and the ultimate regime is not reached for large s data. Figure 3 is a plot of the scaling function $g(x)$ defined above. We find $\lambda' \simeq 2.5$, with $\lambda = 1$.

Let us note that before attaining the intermediate scaling regime there is yet another temporal regime, clearly visible in figures 2 and 3, which takes place at very short times. One can show that in the scaling variable of figure 3 this very short time regime becomes smaller when s increases, and therefore irrelevant in the $s \rightarrow \infty$ limit. Indeed one finds numerically—see figure 4—that in the very short time regime the autocorrelation function can be written as follows:

$$1 - C(t, s) \approx \frac{t - s}{s^{2/3}}. \quad (26)$$

Equation (26) implies that the timescale of decorrelation processes happening in the very short time regime is $s^{2/3}$. This timescale is much smaller than the timescale of the intermediate regime, which is s .

In preparation for section 5, let us mention that, at criticality, dynamical scaling predicts that

$$C(t, 0) \sim L(t)^{-\lambda_c}, \quad (27)$$

defining the critical autocorrelation exponent λ_c [3, 2]. We have also, for s in the scaling regime,

$$C(t, s) \sim L(s)^{-2\beta/\nu} \left(\frac{L(t)}{L(s)} \right)^{-\lambda_c}, \quad (28)$$

where β and ν are the usual static critical exponents ($\beta = 1/4$, $\nu = 1$, in 2D). This form holds for both non-conserved and conserved dynamics, with the possibility that, for the

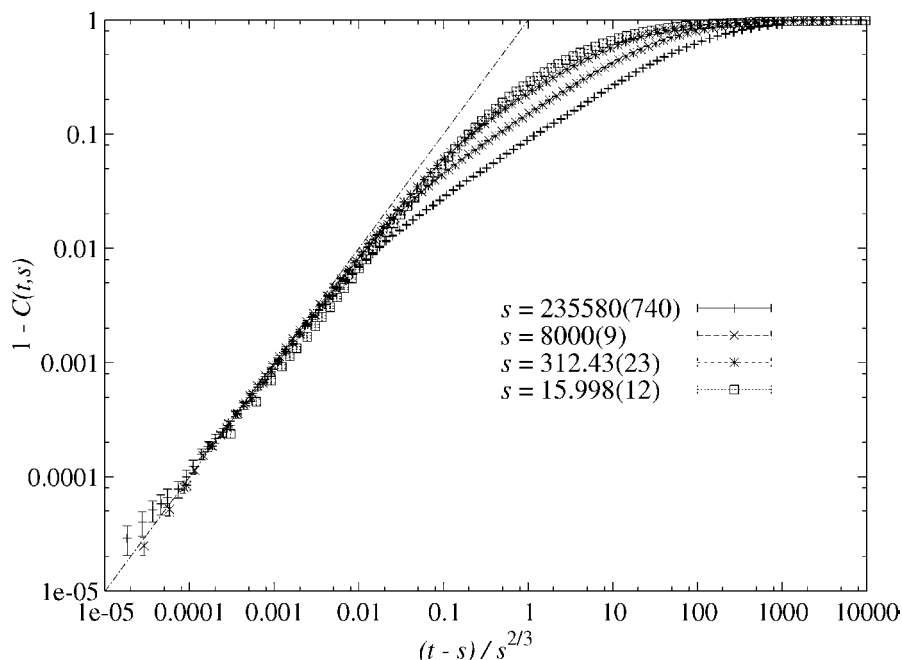


Figure 4. Scaling of the autocorrelation function at very short times.

latter, the exponent appearing in (28) may not be the same as in (27), as discussed in section 5. For conserved dynamics at criticality, [25]–[27] predict $\lambda_c = d$, while statements made in [28] on the long time behaviour of the autocorrelation are less precise.

A last comment is in order. At criticality, there are no well defined growing domains. The interpretation of the growing length in equations (27) and (28) is the typical size over which the system looks critical. The present situation of a system evolving after a quench from high temperature to $T = T_c$ is nevertheless usually referred to as ‘critical coarsening’. By convenience we shall still call the length $L(t)$ the mean domain size.

Note that for the Ising chain the magnetization exponent $\beta = 0$; hence there is no distinction to be made between the two behaviours (20) and (28).

4.3. Response and fluctuation-dissipation plot

Let us recall that for the zero-temperature non-conserved (Glauber) case, the two-time correlation [1] and response functions are known analytically [8, 9]. As a consequence, the fluctuation-dissipation ratio $X(t, s)$, defined by [5]

$$R(t, s) = \frac{X(t, s)}{T} \frac{\partial C(t, s)}{\partial s},$$

can be obtained in closed form. In the scaling regime, it reads

$$X(t, s) \approx \frac{1}{2} \left(1 + \frac{s}{t} \right),$$

yielding, for large temporal separations, the limiting ratio

$$X_\infty = \lim_{s \rightarrow \infty} \lim_{t \rightarrow \infty} X(t, s) = \frac{1}{2}.$$

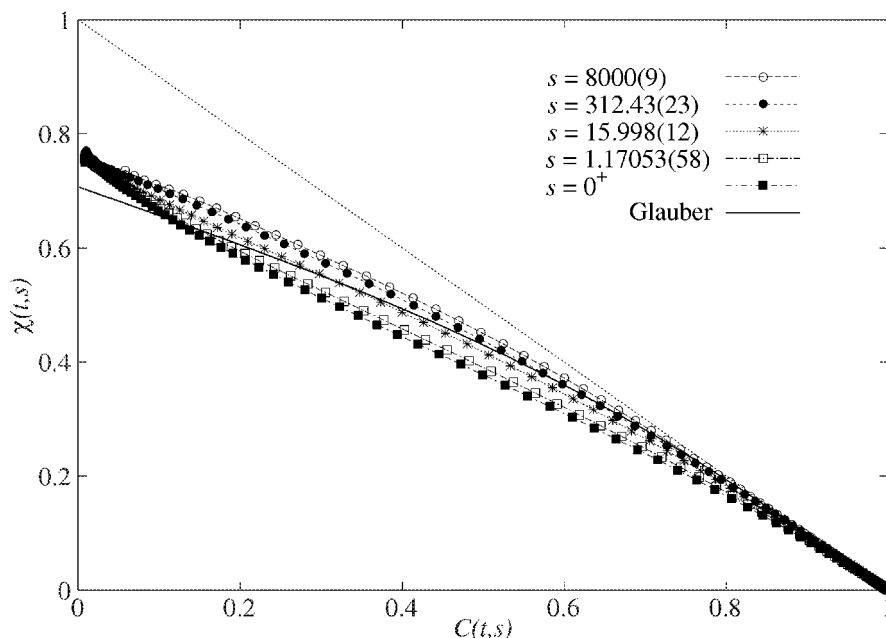


Figure 5. Integrated response against autocorrelation for the Ising–Kawasaki chain at vanishingly small temperature.

In the scaling regime, the integrated response functions $\rho(t, s)$ and $\chi(t, s)$ only depend on t/s , or equivalently on C :

$$\rho(C) = \frac{1}{\sqrt{2}} - \chi(C) = \frac{\sqrt{2}}{\pi} \arctan\left(\frac{1}{\sqrt{2}} \tan \frac{\pi C}{2}\right). \quad (29)$$

Alternatively the limiting ratio can be extracted from $\rho(C)$, as

$$X_\infty = \lim_{C \rightarrow 0} \frac{\rho(C)}{C}. \quad (30)$$

Note that, in contrast to the generic two-dimensional case considered in section 5, for the Ising chain, the integrated response function does not bear any dependence on s because the exponent $\beta = 0$.

We now turn to the Ising–Kawasaki chain. Figure 5 depicts a plot of the integrated response $\chi(t, s)$ against the correlation $C(t, s)$, in the limit of vanishingly small temperature, for the values of the waiting time s given in table 1. Most of the plot corresponds to the intermediate regime ($t \ll t^*(s)$), since the ultimate regime is reached only for the two smallest s values and very small correlations $C(t, s) \lesssim 0.03$ (see figure 2). Restricting to the first regime, we observe a slow convergence of the data to a limiting curve when s increases. However, this limiting curve lies above the theoretical Glauber curve (29), in contradiction with the prediction made in [29], stating that the fluctuation-dissipation plot for the Ising–Kawasaki chain is identical to that of the Ising–Glauber chain, for vanishingly small temperature.

We are thus led to critically review [29]. A similar plot of the integrated response against correlation is presented in this reference, for three sets of values of T and s :

($T = 0.48, s = 3 \times 10^4$), ($T = 0.70, s = 2 \times 10^3$), and ($T = 0.70, s = 10^4$). For these values of (T, s) the data follow rather closely, at least in a range of values of the correlation, the theoretical Glauber curve (29). The authors of [29] therefore deduce that the data obtained for vanishingly small temperatures and increasing values of s should eventually converge to equation (29).

Noting that the values of (T, s) mentioned above correspond, in units of $e^{4\beta}$, to $s = 7.2, 6.6,$ and 33 respectively, we see in figure 5 that, indeed, for this range of values of s , the data points fall not too far away from the Glauber curve. However, since this holds neither for smaller nor for larger values of s (in units of $e^{4\beta}$), we conclude that the apparent identity between the Kawasaki and Glauber curves observed in [29] is just a coincidence due to the range of values considered in this reference.

The existence, in the intermediate regime, of a non-trivial scaling limit for the response implies, as a corollary, a non-trivial value of X_∞ , when the ratio $x = t/s \rightarrow \infty$. A precise numerical value of this quantity is however difficult to obtain from ZFC data. At present we cannot exclude the possibility that X_∞ is the same for both Glauber and Kawasaki dynamics.

Consider now the ultimate regime ($t \gg t^*(s)$). This regime corresponds to $C < \tilde{C}^*(s)$ where $\tilde{C}^*(s) \equiv C(t^*(s), s) \sim s^{-\lambda\lambda' / (\lambda' - \lambda)}$, with $\lambda\lambda' / (\lambda' - \lambda) \simeq 1.66$. This is reminiscent of the situation encountered at criticality for the two-dimensional Ising–Glauber system [10]. In this case the fluctuation-dissipation theorem holds except in a region $C < C^*(s) \sim s^{-a_c}$, where $a_c = 2\beta/\nu z_c \simeq 0.115$, which vanishes for increasing values of s . However, this mechanism does not prevent the occurrence of a non-trivial limiting ratio X_∞ [10] (see section 5). By analogy, we expect a non-trivial value of X_∞ in the ultimate regime, *a priori* different from that obtained in the intermediate regime. Note however that since the exponent $\lambda\lambda' / (\lambda' - \lambda)$ is larger than 1, $\tilde{C}^*(s)$ is decreasing very fast, and, as a consequence, the regime where X_∞ could be measured is hardly reachable in a numerical simulation.

5. Results for the critical dynamics of the 2D Ising–Kawasaki model

The aim of this section is to investigate the critical coarsening of a two-dimensional system of spins evolving under Kawasaki dynamics from a random initial condition. We will, as in the previous section, and inspired by the results found there, examine in turn the behaviour of the two-time correlation function and that of the two-time response function.

5.1. Mean domain length

Numerical study of the long time behaviour of $C(t, s = O(1))$ for the critical dynamics of the 2D Ising–Kawasaki model is well established [26]. Scaling is observed, i.e. equation (27) holds, with a decay exponent $\lambda_c = 2$, confirming the prediction of [25]. The mean domain size itself is observed to grow as $L(t) \sim t^{1/z_c}$, with $z_c = 4 - \eta = 15/4$ [26]. A confirmation of these results is provided by figure 6, where the mean size of domains is extracted from the excess energy with respect to the equilibrium energy at T_c , $E_{\text{eq}} = 1/\sqrt{2}$, i.e. $L(t) = (E(t) - E_{\text{eq}})^{-1}$. This method has already been used for low temperature coarsening, for conserved [37] and non-conserved dynamics [36]. It is however the first time that it is used at criticality, where in general the growing length scale $L(t)$ is obtained

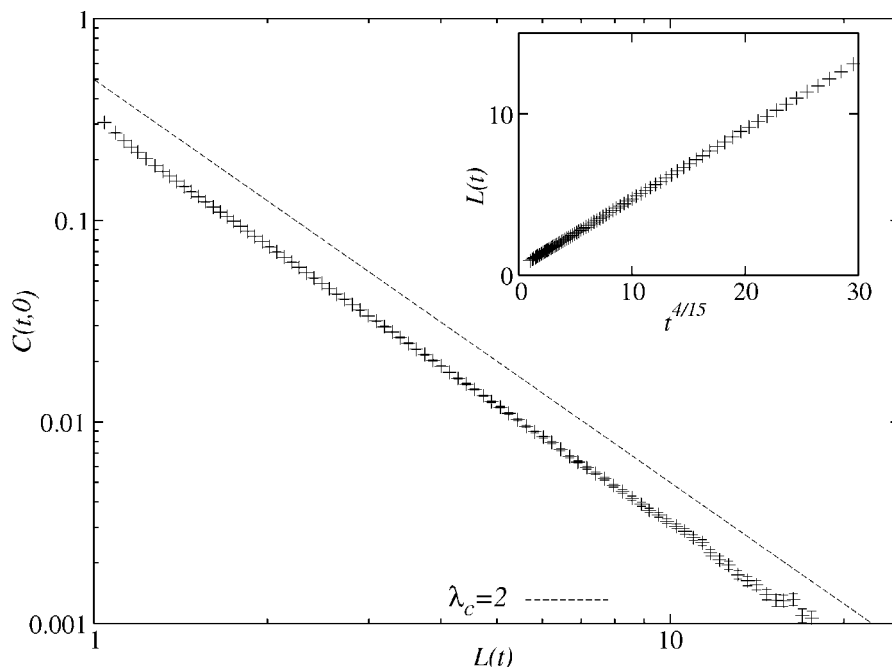


Figure 6. The 2D Ising–Kawasaki model at criticality: $C(t,0)$ and $L(t)$.

from the position of the first zero of the equal-time correlation function. Our reason for doing so lies in the fact that for critical coarsening dynamical scaling holds, as it does for low temperature coarsening, and that therefore there exists only one single growing length scale in the system.

In order to compare the qualitative behaviour of conserved and non-conserved dynamics at T_c , we take a series of snapshots at instants of time where similar domain sizes were reached in the two dynamics (see figure 7). Since for non-conserved dynamics $z_c \approx 2.17$, in 2D, conserved dynamics is much slower. It is interesting to note the overall similarity of the snapshots at corresponding instants of time.

5.2. Autocorrelation

The behaviour of $C(t,s)$ when the waiting time s is deep in the scaling regime is largely unexplored. We first measured the autocorrelation as a function of $L(t)$ for different values of s (see figure 8). As in the one-dimensional case, we observe a seemingly different decay exponent as soon as s becomes large enough, i.e. in this regime equation (28) should be read with a different exponent λ'_c .

In order to assess this point, we define, by analogy with the one-dimensional case (see equation (25)), the scaling function g_c as

$$C(t,s) = L(t)^{-\lambda_c} g_c \left(\frac{L(t)^{\lambda'_c - \lambda_c}}{L(s)^{\lambda'_c - 2\beta/\nu}} \right), \quad (31)$$

with $g_c(x \rightarrow 0) \sim x^{-1}$ in the intermediate regime, while in the ultimate regime $g_c(x \rightarrow \infty)$ should converge to a constant. Figure 9 depicts the scaling function obtained using $\lambda_c = 2$ and $\lambda'_c = 3.5$. In view of this figure it is reasonable to conclude again in favour of the

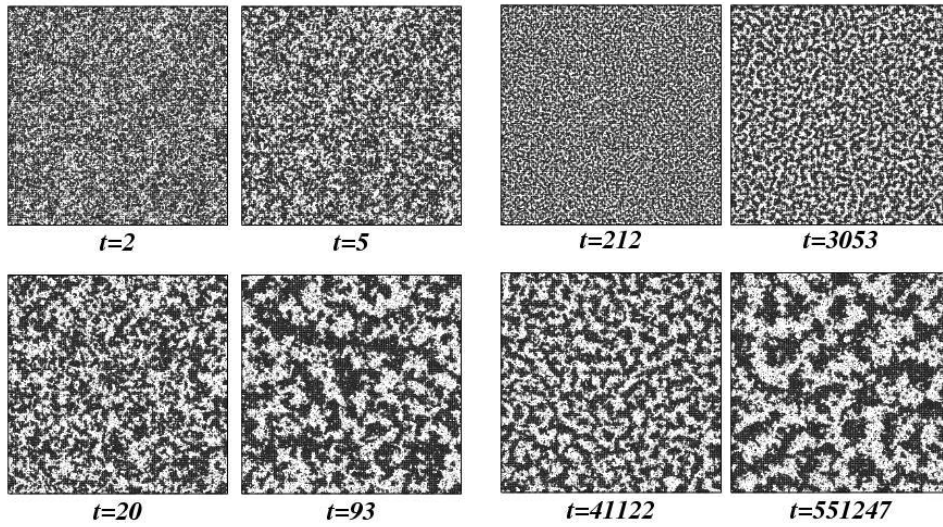


Figure 7. Snapshots of configurations after a quench from $T = \infty$ to T_c in a 500^2 Ising spin system. The four snapshots on the left correspond to Glauber dynamics, while the four on the right correspond to Kawasaki dynamics. Times have been chosen in order to have similar values for $L(t)$.

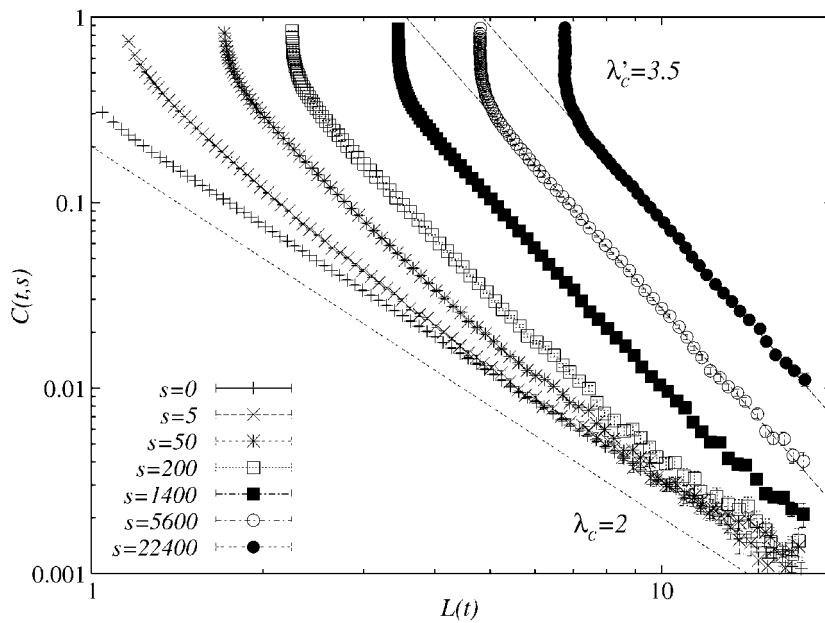


Figure 8. The 2D Ising-Kawasaki model at criticality: $C(t, s)$ against $L(t)$ for different values of s .

existence of these two scaling regimes, defined by the relative magnitude of t with respect to the crossover timescale $t^*(s) \sim s^{(\lambda_c - 2\beta/\nu)/(\lambda_c - \lambda_c)}$. Otherwise stated, $t \ll t^*(s)$ in the intermediate regime, while $t \gg t^*(s)$ in the ultimate regime. We have, with the values of the exponents given above, and $2\beta/\nu = 1/2$, $t^*(s) \sim s^2$.

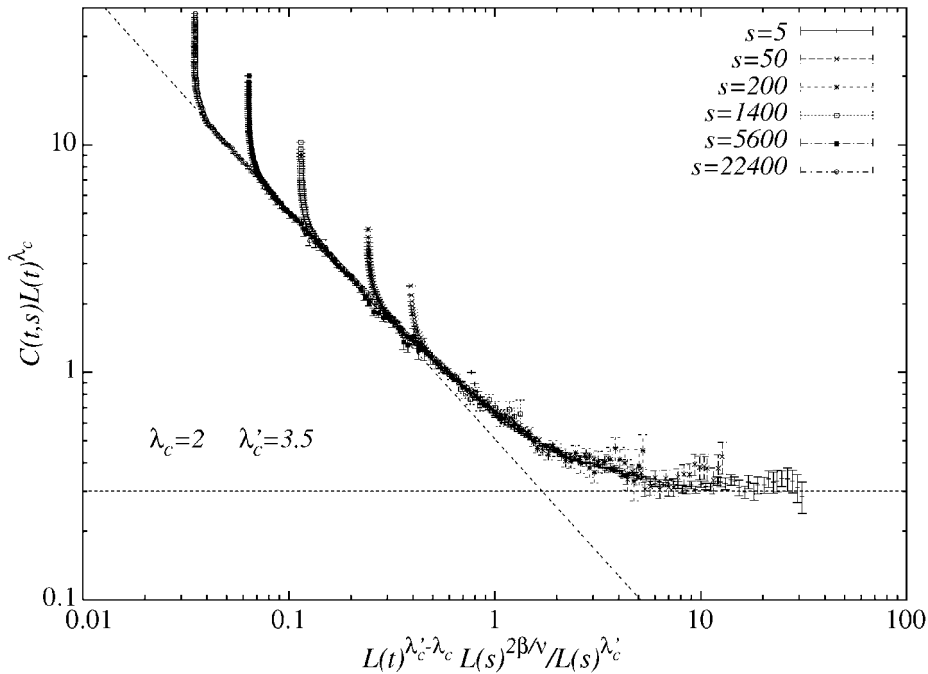


Figure 9. The 2D Ising–Kawasaki model at criticality: the scaling function for the two-time autocorrelation.

5.3. Response and fluctuation-dissipation plot

We now turn to the response. Following [10], we choose to compute the thermoremanent magnetization (14) (TRM). Due to the fast increase of the crossover timescale, $t^*(s) \sim s^2$, and the extreme difficulty of finding precise data for the response at very long times, the results presented below only concern the intermediate regime. These results are contained in figures 10–12.

In the intermediate regime we assume for the TRM a scaling form similar to that of the correlation function, equation (28), that is,

$$\rho(t, s) \sim L(s)^{-2\beta/\nu} \left(\frac{L(t)}{L(s)} \right)^{-\lambda'_c}. \tag{32}$$

This scaling form is well verified by our numerical data, as illustrated by figure 10, which depicts plots of the rescaled correlation and response functions, for both Glauber and Kawasaki dynamics. For the latter, it is interesting to note that, when s increases, the master curve is attained from above for the correlation, and from below for the response, indicating that asymptotically the two scaling functions should have the same algebraic decay with exponent λ'_c . Plots of the scaling functions of autocorrelation and response for the two-dimensional Ising–Glauber model at criticality first appeared in [10]. The value of the exponent measured in the present work is slightly smaller than that found in [10].

Another representation of the same data is given in figure 11, which depicts the parametric plot of the rescaled response against the rescaled correlation, for both Glauber and Kawasaki dynamics. This figure shows that the two dynamics lead to the same phenomenology. Indeed, define a crossover scale for the autocorrelation by $C^*(s) =$

Non-equilibrium critical dynamics of the ferromagnetic Ising model with Kawasaki dynamics

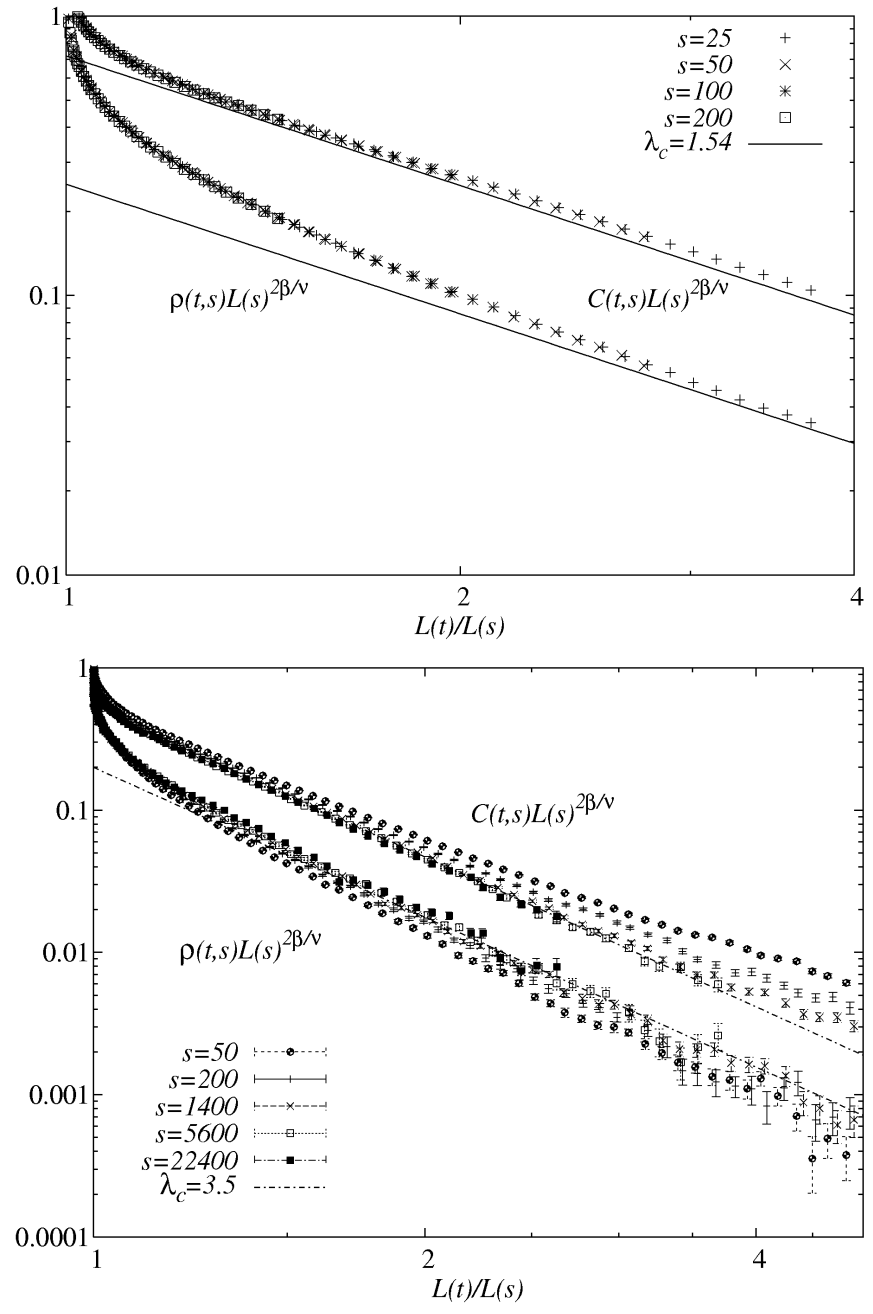


Figure 10. The 2D Ising model at criticality: scaling functions of correlation and response. Top: Glauber dynamics. The full lines have slope $-\lambda_c = -1.54$. Bottom: Kawasaki dynamics. The dotted lines have slope $-\lambda'_c = -3.5$.

$C(2s, s)$ [10], corresponding, for s large enough, to a value of the abscissa on figure 11 approximately equal to 0.47 for Glauber dynamics and to 0.27 for Kawasaki dynamics. Then, on the right part of the plots with respect to these values, the slope of the two curves is equal to one, in agreement with the fluctuation-dissipation theorem. The left part of the plots corresponds to the scaling regime, with a crossover to a non-trivial slope at the origin, equal to the limiting violation ratio X_∞ .

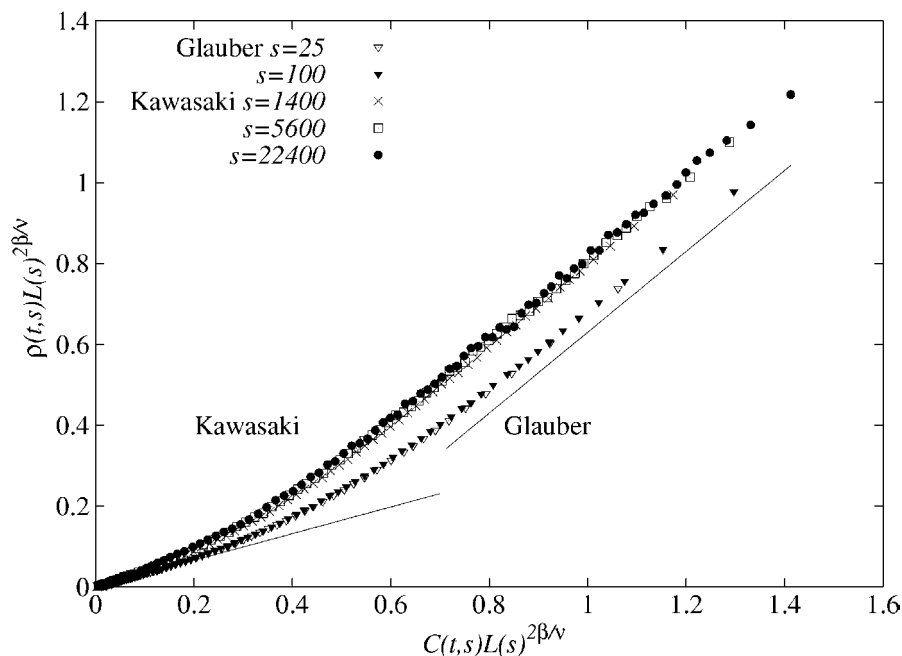


Figure 11. The 2D Ising model at criticality: parametric plots of rescaled response versus rescaled correlation for Glauber and Kawasaki dynamics, using the data of figure 10. The full line at the origin has slope 0.33. The other one has slope 1, and is meant as a guide to the eye.

In order to extract the numerical estimates of these slopes from these data, we plot them in two different fashions, as shown in figure 12. Since $\rho(t, s) \approx X_\infty C(t, s)$ (see (30)), we plot the ratio ρ/C , first versus $L(s)/L(t)$ (figure 12 (top)), then versus the ratio of times s/t (figure 12 (bottom)). Error bars are not shown in the latter, in order to improve clarity. For the Glauber dynamics X_∞ seems to be attained linearly in s/t , which leads, on taking the intercept with the y -axis, to the prediction $X_\infty^{\text{Glauber}} \approx 0.33$, in agreement with the estimates given in recent works [15, 30]. Note that for the spherical model the correction to X_∞ is exactly in s/t [10]. Finally, though it is difficult to be conclusive on the sole basis of figure 12, the latter gives more evidence in favour of different values for the limiting ratios corresponding to the two dynamics, with $X_\infty^{\text{Kawasaki}} > X_\infty^{\text{Glauber}}$.

6. Conclusion

Let us summarize the most salient points of this study.

We extend the method of [30, 31] to the case of Kawasaki dynamics. We introduce a new method for the investigation of the low temperature scaling regime of the Ising–Kawasaki chain. We define rules for an accelerated dynamics, which are both faithful and efficient. This method can be extended to higher dimensions. We find new results concerning the behaviour at large time of the autocorrelation function for the critical Kawasaki dynamics in both dimensionalities, and demonstrate the existence of an ultimate regime, which was overlooked in previous studies. We believe this regime to be also present in the behaviour of the response, though hardly accessible with present computer

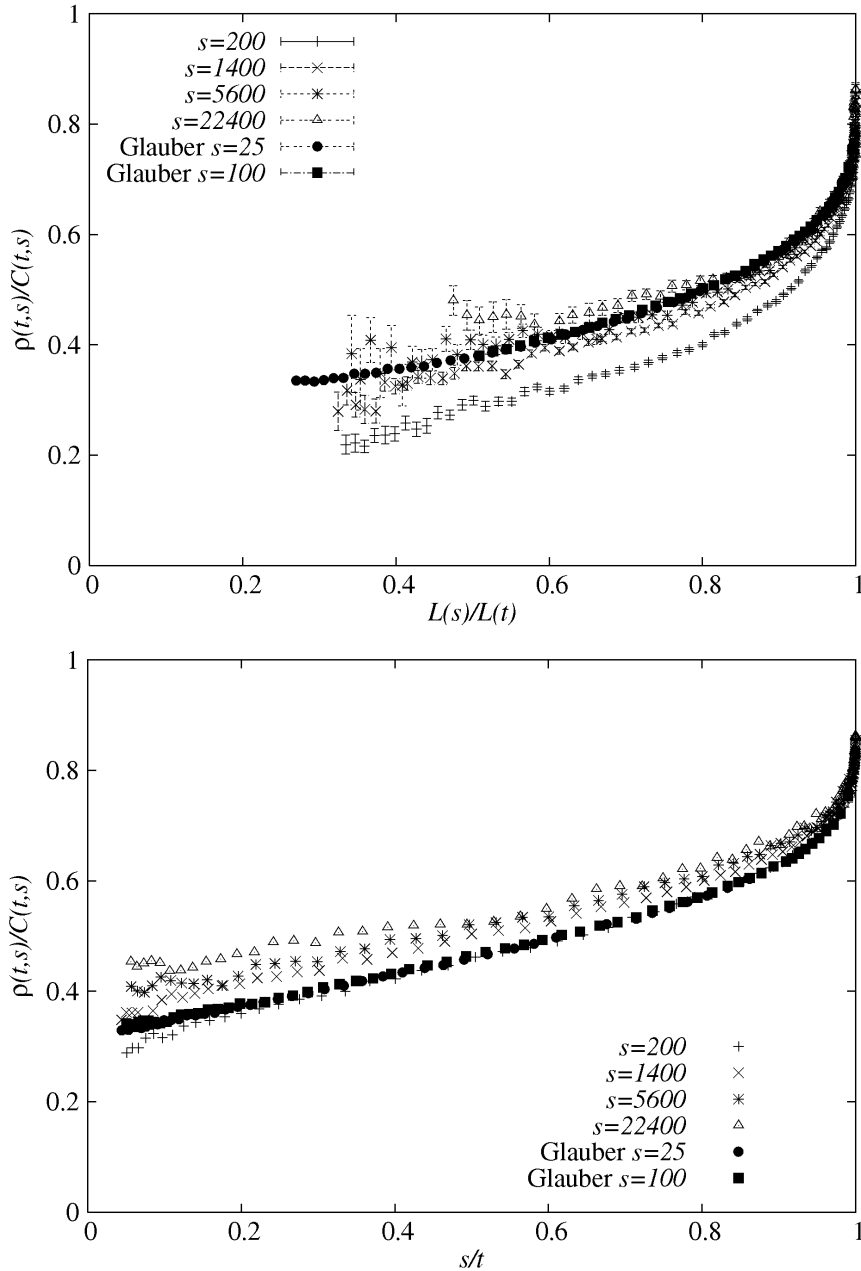


Figure 12. The 2D Ising model at criticality. Top: ρ/C versus $L(s)/L(t)$; bottom: ρ/C versus s/t .

capabilities. As a corollary, we expect the existence of a different value of the limiting ratio X_∞ in the ultimate regime, which would require timescales which are currently unreachable.

In the course of this study we were led to question the validity of the results of [29] concerning the fluctuation-dissipation plot for the Ising–Kawasaki chain. The evidence, claimed in [29], for the identity of the fluctuation-dissipation plots for Glauber and Kawasaki dynamics is seemingly coincidental, and results from the range of values used in this reference.

For the two-dimensional system at criticality, the fluctuation-dissipation plots obtained from the two dynamics are phenomenologically similar, but not quantitatively identical. In particular, the limiting violation ratios X_∞ are found to be different. It is harder though to be conclusive in the two-dimensional case than in the one-dimensional one. In the former, the scaling region defined by $C(t, s) < C^*(s) \sim s^{-0.115}$ is small, while in the latter, since $\beta = 0$, it is identified as the whole range $0 \leq C(t, s) \leq 1$.

In the intermediate scaling regime, numerical data are compatible with the simple form $\lambda'_c = d + 3/2$ for the autocorrelation exponent. It would be interesting to assess the validity of this hypothesis. A theoretical explanation of the existence of the ultimate regime, both for the autocorrelation and for the response, is needed. Finally, a natural extension of the present work is a study of the behaviour of the autocorrelation and response in the low temperature phase ($T < T_c$) of the two-dimensional kinetic Ising model with Kawasaki dynamics.

Acknowledgments

CG wishes to thank Giorgio Parisi for his warm hospitality at the Statistical Mechanics and Complexity Centre, where this work was initiated. FK and FRT acknowledge the financial support provided through the European Community's Human Potential Programme under contracts HPRN-CT-2002-00319, Stipco, and HPRN-CT-2002-00307, Dyglagemem.

References

- [1] Bray A J, 1994 *Adv. Phys.* **43** 357
- [2] Janssen H K, Schaub B and Schmittmann B, 1989 *Z. Phys. B* **73** 539
- [3] Huse D A, 1989 *Phys. Rev. B* **40** 304
- [4] Cugliandolo L F, Kurchan J and Parisi G, 1994 *J. Physique I* **4** 1641
- [5] Cugliandolo L F and Kurchan J, 1994 *J. Phys. A: Math. Gen.* **27** 5749
- [6] Barrat A, 1998 *Phys. Rev. E* **57** 3629
- [7] Berthier L, Barrat J L and Kurchan J, 1999 *Eur. Phys. J. B* **11** 635
- [8] Godrèche C and Luck J M, 2000 *J. Phys. A: Math. Gen.* **33** 1151
- [9] Lippiello E and Zannetti M, 2000 *Phys. Rev. E* **61** 3369
- [10] Godrèche C and Luck J M, 2000 *J. Phys. A: Math. Gen.* **33** 9141
- [11] Henkel M, Pleimling M, Godrèche C and Luck J M, 2001 *Phys. Rev. Lett.* **87** 265701
- [12] Calabrese P and Gambassi A, 2002 *Phys. Rev. E* **65** 066120
- [13] Calabrese P and Gambassi A, 2002 *Phys. Rev. B* **66** 212407
- [14] Picone A and Henkel M, 2002 *J. Phys. A: Math. Gen.* **35** 5575
- [15] Mayer P, Berthier L, Garrahan J P and Sollich P, 2003 *Phys. Rev. E* **68** 016116
- [16] Mayer P and Sollich P, 2004 *J. Phys. A: Math. Gen.* **37** 9
- [17] Crisanti A and Ritort F, 2003 *J. Phys. A: Math. Gen.* **36** R181
- [18] Sastre F, Dornic I and Chaté H, 2003 *Preprint cond-mat/0308178*
- [19] Godrèche C and Luck J M, 2002 *J. Phys.: Condens. Matter* **14** 1589
- [20] Corberi F, Lippiello E and Zannetti M, 2003 *Preprint cond-mat/0307542*
- [21] Pleimling M, 2003 *Preprint cond-mat/0309652*
- [22] Henkel M, Paessens M and Pleimling M, 2003 *Preprint cond-mat/0310761*
- [23] Corberi F, Castellano C, Lippiello E and Zannetti M, 2003 *Preprint cond-mat/0311046*
- [24] Kawasaki K, 1966 *Phys. Rev.* **145** 224
- [25] Majumdar S N, Huse D A and Lubachevsky B D, 1994 *Phys. Rev. Lett.* **73** 182
- [26] Alexander F J, Huse D A and Janowsky S A, 1994 *Phys. Rev. B* **50** 663
- [27] Majumdar S N and Huse D A, 1995 *Phys. Rev. E* **52** 270
- [28] Yeung C, Rao M and Desai R C, 1996 *Phys. Rev. E* **53** 3073
- [29] Corberi F, Lippiello E and Zannetti M, 2002 *Phys. Rev. E* **65** 066114
- [30] Chatelain C, 2003 *J. Phys. A: Math. Gen.* **36** 10739

- [31] Ricci-Tersenghi F, 2003 *Phys. Rev. E* **68** 065104(R)
- [32] Cornell S J, Kaski K and Stinchcombe R B, 1991 *Phys. Rev. B* **44** 12263
- [33] De Smedt G, Godrèche C and Luck J M, 2003 *Eur. Phys. J. B* **32** 215
- [34] Cordery R, Sarker S and Tobochnik J, 1981 *Phys. Rev. B* **24** 5402
- [35] Godrèche C and Luck J M, 2003 *J. Phys. A: Math. Gen.* **36** 9973
- [36] Fisher D S and Huse D A, 1988 *Phys. Rev. B* **38** 373
- [37] Amar J G, Sullivan F E and Mountain R D, 1988 *Phys. Rev. B* **37** 196